

**Involvement of a Binuclear Species with the Re–C(O)O–Re
Moiety in CO₂ Reduction Catalyzed by Tricarbonyl Rhenium(I)
Complexes with Diimine Ligands: Strikingly Slow Formation
of the Re–Re and Re–C(O)O–Re Species from
Re(dmb)(CO)₃S (dmb = 4,4'-Dimethyl-2,2'-bipyridine,
S = Solvent)**

Yukiko Hayashi, Shouichi Kita,[†] Bruce S. Brunshwig,[‡] and Etsuko Fujita*

*Contribution from the Chemistry Department, Brookhaven National Laboratory,
Upton, New York 11973-5000*

Received May 5, 2003; E-mail: fujita@bnl.gov

Abstract: Excited-state properties of *fac*-[Re(dmb)(CO)₃(CH₃CN)]PF₆, [Re(dmb)(CO)₃]₂ (where dmb = 4,4'-dimethyl-2,2'-bipyridine), and other tricarbonyl rhenium(I) complexes were investigated by transient FTIR and UV–vis spectroscopy in CH₃CN or THF. The one-electron reduced monomer, Re(dmb)(CO)₃S (S = CH₃CN or THF), can be prepared either by reductive quenching of the excited states of *fac*-[Re(dmb)(CO)₃(CH₃CN)]PF₆ or by homolysis of [Re(dmb)(CO)₃]₂. In the reduced monomer's ground state, the odd electron resides on the dmb ligand rather than on the metal center. Re(dmb)(CO)₃S dimerizes slowly in THF, $k_d = 40 \pm 5 \text{ M}^{-1} \text{ s}^{-1}$. This rate constant is much smaller than those of other organometallic radicals which are typically $10^9 \text{ M}^{-1} \text{ s}^{-1}$. The slower rate suggests that the equilibrium between the ligand-centered and metal-centered radicals is very unfavorable ($K \approx 10^{-4}$). The reaction of Re(dmb)(CO)₃S with CO₂ is slow and competes with the dimerization. Photolysis of [Re(dmb)(CO)₃]₂ in the presence of CO₂ produces CO with a 25–50% yield based on [Re]. A CO₂ bridged dimer, (CO)₃(dmb)Re–CO(O)–Re(dmb)(CO)₃ is identified as an intermediate. Both [Re(dmb)(CO)₃]₂(OCO₂) and Re(dmb)(CO)₃(OC(O)OH) are detected as oxidation products; however, the previously reported formato-rhenium species is not detected.

Introduction

Photochemical conversion of CO₂ to fuels or useful chemicals using renewable solar energy can contribute to solutions to both the world's needs for fuels and the reduction of greenhouse gases.^{1–3} Rhenium(I) diimine complexes have been shown to act as photocatalysts^{4–12} and/or electrocatalysts^{13–20} for CO₂

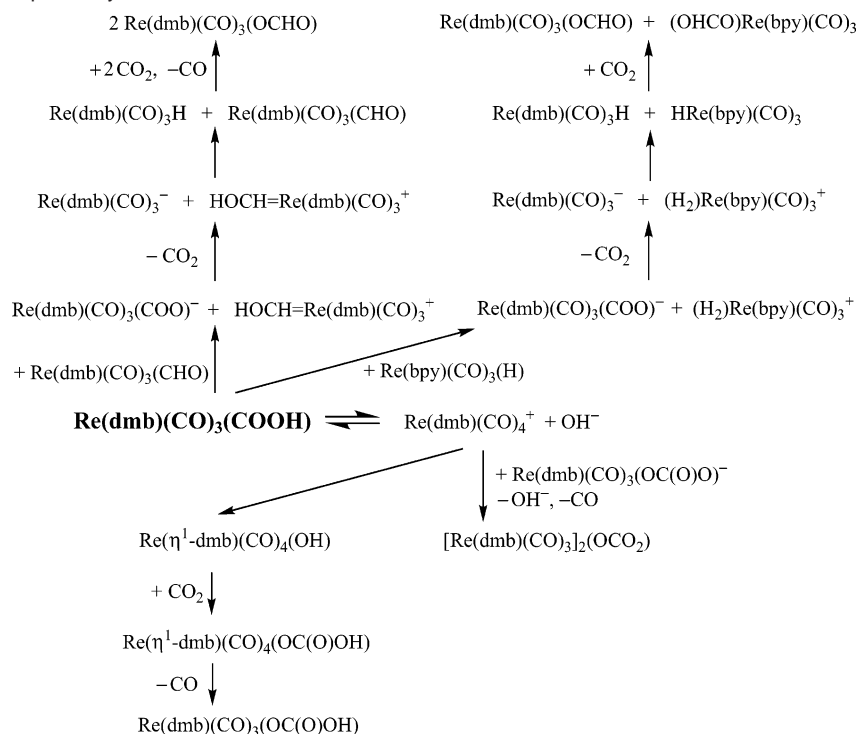
reduction to CO. Metallocarboxylates and metallocarboxylic acids have been proposed as intermediates for CO production,^{1,10,14,18,21} but neither has been observed directly in rhenium(I) catalyzed photochemical or electrochemical systems. For the electrocatalytic reduction of CO₂ to CO with Re(bpy)(CO)₃Cl (bpy = 2,2'-bipyridine), Sullivan et al. proposed two pathways: one involving a one-electron-reduced complex, Re(bpy)(CO)₃, formed by a loss of the Cl[–] ligand and another involving a two-electron-reduced complex, [Re(bpy)(CO)₃][–].¹⁴ Johnson et al. further studied the dependence of the electro-

[†] Current address: Department of Materials Science and Technology, Faculty of Science and Technology, Hirosaki University, Bunkyo-cho 3, Hirosaki, Aomori 036-8561, Japan.

[‡] Current address: Molecular Materials Resource Center, Beckman Institute, MC 139-74, California Institute of Technology, 1200 East California Blvd., Pasadena, CA 91125.

- (1) Sutin, N.; Creutz, C.; Fujita, E. *Comments Inorg. Chem.* **1997**, *19*, 67–92.
- (2) Fujita, E.; Brunshwig, B. S. In *Catalysis of Electron Transfer, Heterogeneous and Gas-Phase Systems*; Fukuzumi, S., Mallouk, T. E., Haas, Y., Eds.; Wiley-VCH: Weinheim, Germany, 2001; Vol. 4, pp 88–126.
- (3) Halmann, M. M.; Steinberg, M. *Greenhouse Gas Carbon Dioxide Mitigation, Science and Technology*; Lewis Publisher: Boca Raton, FL, 1999.
- (4) Hawecker, J.; Lehn, J.-M.; Ziessel, R. *J. Chem. Soc., Chem. Commun.* **1983**, 536–538.
- (5) Hawecker, J.; Lehn, J.-M.; Ziessel, R. *Helv. Chim. Acta* **1986**, *69*, 1990–2012.
- (6) Kutal, C.; Weber, M. A.; Ferraudi, G.; Geiger, D. *Organometallics* **1985**, *4*, 2161–2166.
- (7) Kutal, C.; Corbin, A. J.; Ferraudi, G. *Organometallics* **1987**, *6*, 553–557.
- (8) Hori, H.; Johnson, F. P. A.; Koike, K.; Ishitani, O.; Ibusuki, T. *J. Photochem. Photobiol., A* **1996**, *96*, 171–174.
- (9) Hori, H.; Johnson, F. P. A.; Koike, K.; Takeuchi, K.; Ibusuki, T.; Ishitani, O. *J. Chem. Soc., Dalton Trans.* **1997**, 1019–1023.
- (10) Koike, K.; Hori, H.; Ishizuka, M.; Westwell, J. R.; Takeuchi, K.; Ibusuki, T.; Enjouji, K.; Konno, H.; Sakamoto, K.; Ishitani, O. *Organometallics* **1997**, *16*, 5724–5729.

- (11) Koike, K.; Okoshi, N.; Hori, H.; Takeuchi, K.; Ishitani, O.; Tsubaki, H.; Clark, I. P.; George, M. W.; Johnson, F. P. A.; Turner, J. J. *J. Am. Chem. Soc.* **2002**, *124*, 11448–11455.
- (12) Hori, H.; Ishihara, J.; Koike, K.; Takeuchi, K.; Ibusuki, T.; Ishitani, O. *J. Photochem. Photobiol., A* **1999**, *120*, 119–124.
- (13) Hawecker, J.; Lehn, J.-M.; Ziessel, R. *J. Chem. Soc., Chem. Commun.* **1984**, 328–330.
- (14) Sullivan, B. P.; Bolinger, C. M.; Conrad, D.; Vining, W. J.; Meyer, T. J. *J. Chem. Soc., Chem. Commun.* **1985**, 1414–1416.
- (15) Breikss, A. I.; Abruña, H. D. *J. Electroanal. Chem.* **1986**, *201*, 347–358.
- (16) O'Toole, T. R.; Sullivan, B. P.; Bruce, M. R.-M.; Margerum, L. D.; Murray, R. W.; Meyer, T. J. *J. Electroanal. Chem.* **1989**, *259*, 217–239.
- (17) Klein, A.; Vogler, C.; Kaim, W. *Organometallics* **1996**, *15*, 236–244.
- (18) Johnson, F. P. A.; George, M. W. W.; Hartl, F.; Turner, J. J. *Organometallics* **1996**, *15*, 3374–3387.
- (19) Sullivan, B. P.; Bruce, M. R. M.; O'Toole, T. R.; Bolinger, C. M.; Megehee, E.; Thorp, H.; Meyer, T. J. In *Catalytic Activation of Carbon Dioxide*; Ayers, W. M., Ed.; American Chemical Society: Washington, DC, 1988; Vol. 363, pp 52–90.
- (20) Scheiring, T.; Klein, A.; Kaim, W. *J. Chem. Soc., Perkin Trans. 2* **1997**, 2569–2571.

Scheme 1. Mechanism Proposed by Gibson et al.²¹

catalytic pathways on solvent and on the nature of the Re complex using FTIR spectroscopy.¹⁸ A one-electron-reduced species, $[\text{Re}(\text{dmb})(\text{CO})_3\text{Cl}]^-$ (dmb = 4,4'-dimethyl-2,2'-bipyridine) with a monocoordinated bipyridine, is also proposed to be involved in CO_2 coordination and activation.^{4,15} However, no detailed studies have been published that identify the intermediate CO_2 complexes in these pathways. Furthermore, the published characterizations of the reduced species and some of the possible CO_2 intermediates are inconsistent or confusing.^{2,18,22,23} Gibson et al. isolated a key product $\text{Re}(\text{dmb})(\text{CO})_3(\text{COOH})$ from reaction of $[\text{Re}(\text{dmb})(\text{CO})_4]\text{OTf}$ (OTf = trifluoromethanesulfonate) with aqueous KOH.^{24,25} They observed conversion of $\text{Re}(\text{dmb})(\text{CO})_3(\text{COOH})$ to $(\text{CO})_3(\text{dmb})\text{Re}-\text{CO}(\text{O})-\text{Re}(\text{dmb})(\text{CO})_3$ and suggested that the main pathway involves loss of CO_2 from $\text{Re}(\text{dmb})(\text{CO})_3(\text{COOH})$ to form the hydride species, followed by its reaction with $\text{Re}(\text{dmb})(\text{CO})_3(\text{COOH})$ together with liberation of H_2 . More recently, they²¹ suggested that ionization of $\text{Re}(\text{dmb})(\text{CO})_3\text{COOH}$ to form $\text{Re}(\text{dmb})(\text{CO})_4^+$ and OH^- or its proton transfer to highly basic species may play an important role in the photochemical reduction of CO_2 to CO and formate, as shown in Scheme 1. It is also known that $\text{Re}(\text{dmb})(\text{CO})_4^+$ (or $\text{Re}(\text{bpy})(\text{CO})_4^+$) starts to produce CO 2 μs after excitation with a 355 nm laser pulse and completes within 10 μs in CH_2Cl_2 .²⁶

We have studied these photochemical systems focusing on the identification of intermediates and the bond formation/cleavage reactions between the Re center and CO_2 . We have

produced the one-electron-reduced monomer (i.e., $\text{Re}(\text{dmb})(\text{CO})_3\text{S}$) either by reductive quenching of the excited states of *fac*- $[\text{Re}(\text{dmb})(\text{CO})_3(\text{CH}_3\text{CN})]\text{PF}_6$ or by photoinduced homolysis of $[\text{Re}(\text{dmb})(\text{CO})_3]_2$. We describe (1) the remarkably slow dimerization of $\text{Re}(\text{dmb})(\text{CO})_3\text{S}$; (2) the reaction of $\text{Re}(\text{dmb})(\text{CO})_3\text{S}$ with CO_2 to form a CO_2 -bridged binuclear species $(\text{CO})_3(\text{dmb})\text{Re}-\text{CO}(\text{O})-\text{Re}(\text{dmb})(\text{CO})_3$ as an intermediate in CO formation; and (3) the kinetics and mechanism of reactions involving the CO_2 -bridged binuclear species.

Experimental Section

Materials. The complexes, $\text{Re}(\text{dmb})(\text{CO})_3\text{OTf}$,^{10,24} $\text{Re}(\text{dmb})(\text{CO})_3\text{Cl}$,^{15,27} $\text{Re}(\text{bpy})(\text{CO})_3\text{Cl}$,²⁸ $\text{Re}(\text{dmb})(\text{CO})_3(\text{OCHO})$,²⁹ $\text{Re}(\text{dmb})(\text{CO})_3(\text{OC}(\text{O})\text{OH})$,²⁵ $\text{Re}(\text{dmb})(\text{CO})_3\text{H}$,^{25,30} $(\text{CO})_3(\text{dmb})\text{Re}-\text{CO}(\text{O})-\text{Re}(\text{dmb})(\text{CO})_3$,²⁴ $\text{Re}(\text{dmb})(\text{CO})_3\text{COOH}$,²⁴ and $\text{Re}(4,4'\text{-bpy})_2(\text{CO})_3\text{Cl}$ ^{31,32} (4,4'-bpy = 4,4'-bipyridine), were prepared as previously described and characterized by NMR, UV-vis, and IR spectroscopy. $[\text{Re}(\text{dmb})(\text{CO})_3(\text{CH}_3\text{CN})]\text{PF}_6$ and $[\text{Re}(4,4'\text{-bpy})_2(\text{CO})_3(\text{CH}_3\text{CN})]\text{PF}_6$ were prepared by following the procedure for $[\text{Re}(\text{bpy})(\text{CO})_3(\text{CH}_3\text{CN})]\text{PF}_6$.²⁸ $\text{Re}(\text{bpy})(\text{CO})_3(\text{O}^{13}\text{CHO})$ and $\text{Re}(\text{dmb})(\text{CO})_3(\text{O}^{13}\text{CHO})$ were prepared from the corresponding Re–H species with $^{13}\text{CO}_2$.²⁹ $[\text{Re}(\text{dmb})(\text{CO})_3]_2(\text{OCO}_2)$ was isolated from DMF solutions used for photochemical CO_2 reduction with $[\text{Re}(\text{dmb})(\text{CO})_3]_2$ or $[\text{Re}(\text{dmb})(\text{CO})_3]_2(\text{CO}_2)$: FAB-mass (positive): m/z 969 (parent + H^+); Anal. Calcd for $\text{C}_{31}\text{H}_{24}\text{N}_4\text{O}_9\text{Re}_2$: C, 38.43; H, 2.50; N, 5.78. Found: C, 37.75; H, 2.46; N, 5.87%; IR (DMF or *d*₇-DMF): 2011, 1899, 1871 (br) cm^{-1} (ν_{CO}). IR (KBr): ν_{CO} at 2019, 1894, 1869, and 1853; ν_{dmb} at 1622; $\nu_{\text{O}^{13}\text{COO}}$ at 1576, 1288, and 1269; $\nu_{\text{O}^{13}\text{COO}}$ at 1534, 1262, and 1238 cm^{-1} . ^1H NMR (*d*₇-DMF, rt): δ 8.75–

(21) Gibson, D. H.; Yin, X.; He, H. Y.; Mashuta, M. S. *Organometallics* **2003**, *22*, 337–346.

(22) Christensen, P.; Hamnett, A.; Muir, A. V. G.; Timney, J. A. *J. Chem. Soc., Dalton Trans.* **1992**, 1455–1463.

(23) Stor, G. J.; Hartl, F.; Outersterp, J. W. M. V.; Stufkens, D. J. *Organometallics* **1995**, *14*, 1115–1131.

(24) Gibson, D. H.; Yin, X. *J. Am. Chem. Soc.* **1998**, *120*, 11200–11201.

(25) Gibson, D. H.; Yin, X. *J. Chem. Soc., Chem. Commun.* **1999**, 1411–1412.

(26) Bernhard, S.; Omberg, K. M.; Strouse, G. F.; Schoonover, J. R. *Inorg. Chem.* **2000**, *39*, 3107–3110.

(27) Wrighton, M.; Morse, D. L. *J. Am. Chem. Soc.* **1974**, *96*, 998–1003.

(28) Casper, J. P.; Meyer, T. J. *J. Am. Chem. Soc.* **1983**, *87*, 952–957.

(29) Sullivan, B. P.; Meyer, T. J. *J. Chem. Soc., Chem. Commun.* **1984**, 1224–1245.

(30) Sullivan, B. P.; Meyer, T. J. *Organometallics* **1986**, *5*, 1500–1502.

(31) Giordano, P. J.; Wrighton, M. S. *J. Am. Chem. Soc.* **1979**, *101*, 2888–2897.

(32) Gamelin, D. R.; George, M. W.; Glyn, P.; Grevels, F.-W.; Johnson, F. P. A.; Klotzbucher, W.; Morrison, S. L.; Russell, G.; Schaffner, K.; Turner, J. J. *Inorg. Chem.* **1994**, *33*, 3246–3250.

8.68 (4H, d, $J = 5.6$ Hz), 8.37–8.03 (4H, s), 7.46–7.26 (4H, d, $J = 5.6$ Hz), 2.42–2.10 (12H, s). The solubility of $[\text{Re}(\text{dmb})(\text{CO})_3]_2(\text{OCO}_2)$ in DMF is limited, and the NMR signals shift during the solid formation. ^{13}C NMR (d_7 -DMF, rt): δ 200.7, 196.9, 166.7 (OCO_2), 156.2, 152.8, 152.6, 129.2, 128.7, 21.7. While our IR results for $[\text{Re}(\text{dmb})(\text{CO})_3]_2(\text{OCO}_2)$ are not in agreement with recent published results,²¹ we confirmed our assignment by the ^{13}C isotope replacement studies.

Acetonitrile (CH_3CN) and tetrahydrofuran (THF) were purified in the published manner³³ and stored under vacuum over activated molecular sieves (MS) and sodium–potassium alloy (NaK), respectively. Triethylamine (TEA) was distilled with NaK. Dimethylformamide (DMF) was distilled with CaH_2 and stored in an Ar-filled glovebox. d_7 -DMF was used after drying over activated MS unless mentioned otherwise. Research grade CO_2 ($\text{CO}_2 > 99.998\%$) was used without further purification. $^{13}\text{CO}_2$ was dried over P_2O_5 and purified by freeze–thaw cycles to remove other gaseous impurities.

Preparation of Reduced $\text{Re}(\text{dmb})(\text{CO})_3\text{X}$ by Na–Hg or Na Mirror. Solutions of the reduced species (0.04–3 mM) were prepared under vacuum by either sodium amalgam (Na–Hg, 0.5% Na in Hg) in CH_3CN or Na mirror reduction in THF in sealed glassware equipped with an optical cell and/or an NMR tube. After removing the chamber containing Na–Hg or Na mirror by flame seal, we introduced 1 atm of CO_2 into the cell. For NMR measurements of $[\text{Re}(\text{dmb})(\text{CO})_3]^-$, the NMR tube was flame-sealed after the UV–vis spectrum was measured using a 0.1 mm optical cell. Dark solid $[\text{Re}(\text{dmb})(\text{CO})_3]_2$ was prepared from a THF solution containing $\text{Re}(\text{dmb})(\text{CO})_3\text{OTf}$ by Na–Hg reduction. The solids were collected, washed with THF, and stored in an argon-filled glovebox. Since $[\text{Re}(\text{dmb})(\text{CO})_3]_2$ and all other reduced species are air- and moisture-sensitive, the solutions for physical measurements were prepared with great care using very dry solvents. The DMF solutions containing $[\text{Re}(\text{dmb})(\text{CO})_3]_2$ were prepared in a glovebox, and all other solutions were prepared using a vacuum line.

Spectroscopic Measurements. UV–vis spectra were measured on a Hewlett-Packard 8452A diode array spectrophotometer. FTIR spectra were measured on a Mattson Polaris FT-IR spectrometer or a Bruker IFS 66/s spectrometer. NMR spectra were measured on a Bruker UltraShield 400 MHz spectrometer. Transient UV–vis absorption spectra and lifetimes of various intermediates were measured using a modified apparatus described elsewhere.^{34,35} Excitation was provided by the third (355 nm, ~ 6 ns) or second harmonic (532 nm, ~ 6 ns) of a Continuum Surelite-1 Nd:YAG laser. Flash photolysis experiments of $[\text{Re}(\text{dmb})(\text{CO})_3]_2$ in THF were performed at 15 °C under vacuum or with 1 atm of CO . All CW experiments were performed at 25 °C under vacuum or with 1 atm of Ar or CO_2 . The kinetics of the signal-averaged data were analyzed using Levenberg–Marquardt nonlinear least-squares routines written in MATLAB. Transient FTIR spectra of Re complexes were measured using a Bruker IFS 66/s spectrometer with a Kolmar HgCdTe detector and a flow cell (1.0–2.8 mm path length) for step scan (time resolution: 10 ns) or with a Graseby infrared photoconductive HgCdTe detector and a 0.1–0.5 mm path length vacuum tight cell for rapid scan. Acetonitrile solutions containing 1–2 mM Re complex with or without 1 M TEA were bubbled by Ar or CO_2 for at least 10 min before measurements. The sample was excited with the third harmonic (355 nm, 6 ns) of a Continuum Surelite-1 Nd:YAG laser. The excitation energy was typically 20 mJ cm^{-2} per pulse.

Continuous Photolysis. Solutions were prepared under either vacuum or 1 atm of Ar or CO_2 and irradiated using light from a 150 W xenon lamp with a 380 nm LP filter. Gaseous products, CO and H_2 ,

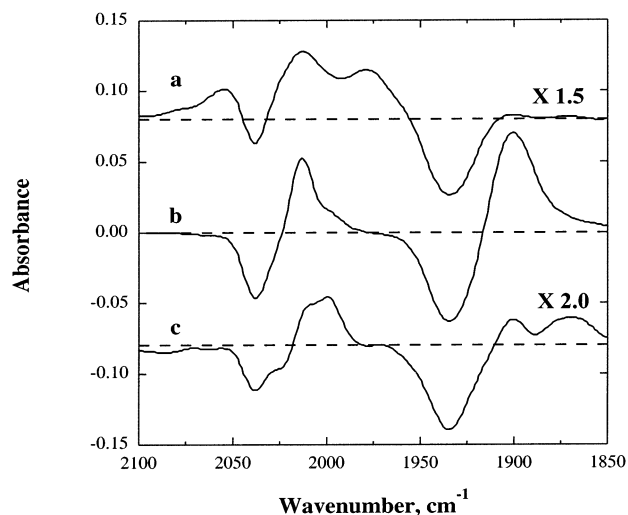


Figure 1. Transient FTIR (difference) spectra of the CH_3CN solution containing $[\text{Re}(\text{dmb})(\text{CO})_3(\text{CH}_3\text{CN})]\text{PF}_6$: (a) the excited-state spectrum under Ar; (b) the photoformed singly reduced species with TEA under Ar; (c) the photoformed one-electron-reduced species with TEA under CO_2 .

were determined on a Varian Model 3700 gas chromatograph equipped with a thermal conductivity detector and a molecular sieve 5A column at 60 °C using He and Ar, respectively, as carrier gases. The other products were analyzed by NMR, FTIR, elemental analysis and/or FAB-mass.

Electrochemistry. Cyclic voltammograms were obtained using a BAS100 electrochemical system with scan rates of 100 mV s^{-1} . The solutions used contained 1 mM rhenium complex and 0.1 M tetrabutylammonium hexafluorophosphate in CH_3CN . Glassy carbon, Pt, and SCE were used as working, counter, and reference electrodes, respectively, in a conventional H-type cell. Ferrocene was used as an internal standard (Fc/Fc^+ 0.39 V vs SCE). The electrochemical behavior of $\text{Re}(\text{diimine})(\text{CO})_3\text{X}$ in the positive region shows one wave; however, in the negative region it shows several reduction waves as previously found.

Results and Discussion

FTIR Studies of Excited States. The transient FTIR spectrum of $[\text{Re}(\text{dmb})(\text{CO})_3(\text{CH}_3\text{CN})](\text{PF}_6)$ in CH_3CN at room temperature following 355 nm laser excitation is shown in Figure 1a. Excitation of $[\text{Re}(\text{dmb})(\text{CO})_3(\text{CH}_3\text{CN})](\text{PF}_6)$ produces the $^3\text{MLCT}$ excited states (to be denoted with an asterisk): The CO stretching bands of $^*[\text{Re}(\text{dmb})(\text{CO})_3(\text{CH}_3\text{CN})]^+$ grow (2062, 2013, and 1979 cm^{-1}), and so do those of the ground-state bleach (2039 and 1934 cm^{-1}). Ground- and excited-state ν_{CO} frequencies for $\text{Re}(\text{bpy})(\text{CO})_3\text{Cl}$ ($\text{bpy} = 2,2'$ -bipyridine), $[\text{Re}(\text{bpy})(\text{CO})_3(\text{CH}_3\text{CN})](\text{PF}_6)$, $\text{Re}(4,4'\text{-bpy})_2(\text{CO})_3\text{Cl}$ ($4,4'$ -bpy = $4,4'$ -bipyridine), $[\text{Re}(4,4'\text{-bpy})_2(\text{CO})_3(\text{CH}_3\text{CN})](\text{PF}_6)$, $\text{Re}(\text{dmb})(\text{CO})_3\text{Cl}$, and $[\text{Re}(\text{dmb})(\text{CO})_3(\text{CH}_3\text{CN})](\text{PF}_6)$ species are listed in Table 1. Assignments of ν_{CO} frequencies were made as described previously.³⁶ The overlapping E mode bands in the ground states of the acetonitrile complexes are resolved into separate $A'(2)$ and A'' bands in the excited states. Upon excitation, three ν_{CO} bands show a 20–90 cm^{-1} shift to higher energy with $A'(2)$ modes having the largest ν_{CO} shift for all complexes studied. In the $^3\text{MLCT}$ excited state, charge has

(33) Riddick, J. A.; Bunger, W. B.; Sakano, T. K. *Organic Solvents, Physical Properties and Methods of Purification*, 4th ed.; Wiley: New York, 1986.

(34) Hamada, T.; Brunschwig, B. S.; Eifuku, E.; Fujita, E.; Korner, M.; Sasaki, S.; van Eldik, R.; Wishart, J. F. *J. Phys. Chem. A* **1999**, *103*, 5645–5654.

(35) Thompson, D. W.; Wishart, J. F.; Brunschwig, B. S.; Sutin, N. *J. Phys. Chem. A* **2001**, *105*, 8117–8122.

(36) Dattelbaum, D. M.; Omberg, K. M.; Schoonover, J. R.; Martin, R. L.; Meyer, T. J. *Inorg. Chem.* **2002**, *41*, 6071–6079.

Table 1. ν_{CO} Frequencies (cm^{-1}) of Ground-State ($\nu_{\text{CO}}(\text{gs})$), Excited-State ($\nu_{\text{CO}}(\text{ex})$), and Photochemically Produced Reduced Species ($\nu_{\text{CO}}(\text{red})$) for Rhenium Complexes in CH_3CN at 298 K

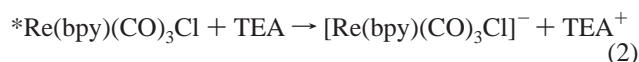
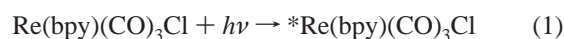
complex	electron donor	$\nu_{\text{CO}}(\text{gs})$			$\nu_{\text{CO}}(\text{ex})$			$\nu_{\text{CO}}(\text{red})$		
		A'(1) or A ₁	A'(2) or E	A''	A'(1)	A'(2)	A''	A'(1) or A ₁	A'(2) or E	A''
Re(bpy)(CO) ₃ Cl	TEA	2023	1914	1902	2068	1989	1957	1998	1880	1866
[Re(bpy)(CO) ₃ (CH ₃ CN)] ⁺	TEA	2040	1937(br)		2070	2017	1987	2017	1902(br)	
	PTZ	2040	1937(br)					2015	1904(br)	
Re(4,4'-bpy) ₂ (CO) ₃ Cl	PTZ	2026	1919	1893	2065	1993	1961	2017	1908	1879
[Re(4,4'-bpy) ₂ (CO) ₃ (CH ₃ CN)] ⁺	PTZ	2046	1942(br)		2068	2031	1992	2015	1904(br)	1879
Re(dmb)(CO) ₃ Cl	TEA	2021	1914	1898	2062	1989	1953			
[Re(dmb)(CO) ₃ (CH ₃ CN)] ⁺	TEA	2039	1934(br)		2062	2013	1979	2012	1904(br)	

transferred from the Re center to the diimine ligand. The decreased charge density on the Re center reduces the π -back-bonding between the Re center and the CO ligands. This in turn increases the CO bond strength and vibration frequencies. Similar effects have been observed in time-resolved resonance Raman spectroscopy studies of similar complexes.³⁷ The ν_{CO} values for *Re(bpy)(CO)₃Cl and *Re(4,4'-bpy)₂(CO)₃Cl are consistent with those reported previously in CH₂Cl₂.^{32,38–40} The lifetimes of *Re(4,4'-bpy)₂(CO)₃Cl and *Re(bpy)(CO)₃Cl observed in our FTIR experiments are 400 ns and 30 ns, respectively, in CH₃CN and are consistent with those obtained by emission measurements at 25 °C.^{31,41}

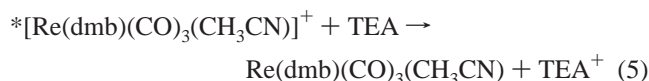
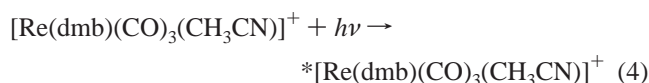
Transient FTIR Studies of One-Electron-Reduced Species.

The ³MLCT excited state of Re(diimine)(CO)₃X is known to be both a strong oxidant and a strong reductant,^{41,42} and it can be quenched by either electron acceptors or donors. In our experiments, *Re(bpy)(CO)₃Cl reacts with electron donors such as triethylamine (TEA) to produce the one-electron-reduced species [Re(bpy)(CO)₃Cl][−] (ν_{CO} : 1998, 1880, 1866 cm^{-1}) in CH₃CN as shown in eqs 1 and 2 and in Table 1. [Re(bpy)(CO)₃Cl][−] has been assigned as a ligand radical with the “added” electron, primarily residing in the bpy- π^* -orbital.^{17,20,43} This increases the charge density on the Re(I) center, since bpy[−] is both a more powerful σ -donor and a poorer π -acceptor (it will not back-bond as well with the Re center). This in turn increases the Re–CO π -back-bonding and the electron density in the π^* -orbital of the CO. This decreases the CO bond strength and shifts ν_{CO} to lower energy by $\sim 30 \text{ cm}^{-1}$. Further, the UV–vis spectra of the one-electron-reduced species [Re(bpy)(CO)₃Cl][−] shows two bands at 486 and 512 nm (in THF) that are similar to the bpy[−] spectra seen in *Re(bpy)(CO)₃Br.⁴⁴ Alternatively, if the added electron were located on the Re center, yielding a Re(0) center that is much more electron rich, one might expect a shift of ν_{CO} to lower energy that is larger than that observed on going from excited (Re^{II}bpy[−]) to the ground (Re^Ibpy) state of Re(bpy)(CO)₃Cl ($\sim 60 \text{ cm}^{-1}$). This assignment is also supported by density functional theory (DFT) calculations that will be published separately.⁴⁵

The transient FTIR spectra show that [Re(bpy)(CO)₃Cl][−] lives longer than 10 ms ($k < 10^2 \text{ s}^{-1}$), thus loss of Cl[−] is slow (eq 3a or 3b) as found previously.^{18,38} The transient FTIR spectrum of [Re(bpy)(CO)₃Cl][−] is identical under Ar and CO₂ indicating that CO₂ does not react with [Re(bpy)(CO)₃Cl][−] on this time scale.



The results of transient FTIR spectra of other rhenium species in CH₃CN are shown in Table 1. Phenothiazine (PTZ) was also used as a reversible one-electron donor. The stability of the reduced complex depends on the ability of the X ligand (X = Cl, Br, H, etc.) and the diimine ligand to accommodate the increased electron density of the Re center.¹⁸ For ligands that cannot accept charge density into a low energy orbital, the Re–X bond is weakened. This can lead to loss of X[−]. Johnson et al. concluded that complexes such as Re(dmb)(CO)₃X tend to form the five-coordinate Re(dmb)(CO)₃ species upon one-electron reduction even in CH₃CN, since dmb is a more basic ligand than bpy.¹⁸



Therefore, we quenched the excited state of [Re(dmb)(CO)₃(CH₃CN)]⁺ with TEA (eqs 4 and 5) in order to create a vacant site for CO₂ coordination. The species produced, which lives longer than 10 ms, has ν_{CO} at 2012 and 1904 (br) cm^{-1} (Figure 1b and Table 1). We propose that this species is a six-coordinate Re(dmb)(CO)₃S (S = solvent) species and not the five-coordinate Re(dmb)(CO)₃ species assigned by Johnson et al.¹⁸

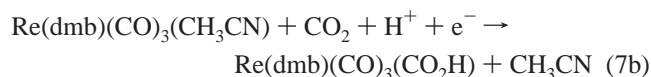
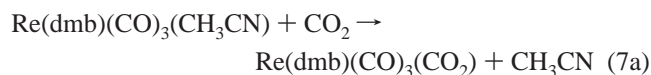
- (37) Stufken, D. J.; Vlcek, A. J. *Coord. Chem. Rev.* **1998**, *177*, 127–179.
 (38) George, M. W.; Johnson, F. P. A.; Westwell, J. R.; Hodges, P. M.; Turner, J. J. *J. Chem. Soc., Dalton Trans.* **1993**, 2977–2979.
 (39) George, M. W.; Turner, J. J. *Coord. Chem. Rev.* **1998**, *177*, 201–217.
 (40) Glyn, P.; George, M. W.; Hodges, P. M.; Turner, J. J. *J. Chem. Soc. Chem. Commun.* **1989**, 1655–1657.
 (41) Kalyanasundaram, K. *J. Chem. Soc., Faraday Trans.* **1986**, *82*, 2401–2415.
 (42) Luong, J. C.; Nadjo, L.; Wrighton, M. S. *J. Am. Chem. Soc.* **1978**, *100*, 5790–5795.
 (43) Kaim, W.; Kohlmann, S. *Chem. Phys. Lett.* **1987**, *139*, 365–369.
 (44) Rossenaar, B. D.; Stufkens, D. J.; Vlcek, A. *Inorg. Chim. Acta* **1996**, *247*, 247–255.

- (45) We have carried out DFT and fully ab initio calculations on Re(bpy)(CO)₃, [Re(bpy)(CO)₃Cl][−], and Re(bpy)(CO)₃(THF). The unpaired electron in the HOMO of Re(bpy)(CO)₃ is partially delocalized onto the bpy π system, but it is available for bonding to reform the dimer. In [Re(bpy)(CO)₃Cl][−] and Re(bpy)(CO)₃(THF), the unpaired electron is shifted completely onto the bpy π system. The binding energies of Cl[−] and THF are 22 and 18 kcal/mol, respectively, and these six-coordinate 18 e[−] ligand radical species are more stable than the five-coordinate “17 e[−]” species. Detailed results will be published in a forthcoming paper (in preparation with J. T. Muckerman, BNL).

A five-coordinate $\text{Re}(\text{dmb})(\text{CO})_3$ species would be either a $16e^-$ species with an unpaired electron located on the dmb ligand or a $17e^-$ species with an unpaired electron located on the metal. According to our recent DFT calculations, $\text{Re}(\text{bpy})(\text{CO})_3(\text{THF})$, which is an $18e^-$ species with an unpaired electron on bpy, is more stable than the five-coordinate $\text{Re}(\text{bpy})(\text{CO})_3$ species.⁴⁵ In fact, the CO stretching frequencies and the maxima of the UV–vis spectra of $\text{Re}(\text{dmb})(\text{CO})_3\text{S}$ are remarkably solvent dependent, consistent with the solvent coordination. ν_{CO} (cm^{-1}) 2007, 1897 (br) in THF;⁴⁶ 2012, 1904 (br) in CH_3CN ; 2016, 1910 (br) in DMF. λ_{max} (nm) 356, 467, 496 in THF; 400, 482, 508 in CH_3CN ; 490, 520 in DMF. Furthermore, the UV–vis spectra of $\text{Re}(\text{dmb})(\text{CO})_3(\text{CH}_3\text{CN})$ and $[\text{Re}(\text{dmb})(\text{CO})_3\text{Cl}]^-$ (which has been considered as a ligand radical^{17,20,43}) in CH_3CN are very similar except for small shifts of absorption maxima. λ_{max} for $[\text{Re}(\text{dmb})(\text{CO})_3\text{Cl}]^-$ 486, 512 nm.

The $[\text{Re}(\text{dmb})(\text{CO})_3(\text{CH}_3\text{CN})]^+$ ground state reacts slowly with TEA to form $[\text{Re}(\text{dmb})(\text{CO})_3(\text{TEA})]^+$ (ν_{CO} 2011, 1900 (br) cm^{-1}) in CH_3CN in the dark. Further transient FTIR spectra (not shown) of a solution of $[\text{Re}(\text{dmb})(\text{CO})_3(\text{CH}_3\text{CN})]^+$ containing TEA that was aged 2 h before laser excitation indicates shoulders around 2000 and 1870 cm^{-1} , which can be attributed to $\text{Re}(\text{dmb})(\text{CO})_3(\text{TEA})$, in addition to ν_{CO} at 2012 and 1904 cm^{-1} for $\text{Re}(\text{dmb})(\text{CO})_3(\text{CH}_3\text{CN})$. Such an amine adduct, $[\text{Re}(\text{bpy})(\text{CO})_3(\text{TEOA})]^+$ (TEOA = triethanol amine), has been detected in photochemical CO_2 reduction.⁹

In transient FTIR experiments under CO_2 (CH_3CN , 1 M TEA), we observed the formation of $\text{Re}(\text{dmb})(\text{CO})_3(\text{CH}_3\text{CN})$ (ν_{CO} at 2012 and 1904 cm^{-1}) and another component (ν_{CO} at 2000 and 1868 cm^{-1}), together with loss of $[\text{Re}(\text{dmb})(\text{CO})_3(\text{CH}_3\text{CN})]^+$ and a species which has ν_{CO} at 2022 cm^{-1} , shown in Figure 1c. All signals due to the products (shown as peaks in Figure 1c) remain unchanged for 10 ms. These additional peaks, very similar to those of $[\text{Re}(\text{dmb})(\text{CO})_3(\text{TEA})]^+$ and $\text{Re}(\text{dmb})(\text{CO})_3(\text{TEA})$, were always observed, even when the solution was prepared just before excitation under CO_2 . Signal intensities of $\text{Re}(\text{dmb})(\text{CO})_3(\text{CH}_3\text{CN})$ under CO_2 are weaker than those under Ar. This is due to formation and precipitation of $\text{Re}(\text{dmb})(\text{CO})_3(\text{OC}(\text{O})\text{OH})$ during the transient FTIR experiments. Carbonyl stretching frequencies of $\text{Re}(\text{dmb})(\text{CO})_3(\text{OC}(\text{O})\text{OH})$ and $[\text{Re}(\text{dmb})(\text{CO})_3(\text{TEA})]^+$ are very similar in DMF, as are those of $[\text{Re}(\text{dmb})(\text{CO})_3(\text{OC}(\text{O})\text{OH})]^-$ and $\text{Re}(\text{dmb})(\text{CO})_3(\text{TEA})$. Small amounts of water in the presence of TEA and CO_2 produce $\text{OC}(\text{O})\text{OH}^-$ ions (eq 6), and $\text{Re}(\text{dmb})(\text{CO})_3(\text{OC}(\text{O})\text{OH})$ is formed by reaction of $[\text{Re}(\text{dmb})(\text{CO})_3(\text{CH}_3\text{CN})]^+$ and bicarbonate.



Therefore, the shoulder at 2022 cm^{-1} is assigned for $\text{Re}(\text{dmb})(\text{CO})_3(\text{OC}(\text{O})\text{OH})$. The stretching frequencies at 2000 and 1868 cm^{-1} (Figure 1c) are attributed to $[\text{Re}(\text{dmb})(\text{CO})_3(\text{OC}(\text{O})\text{OH})]^-$.

The IR spectrum of an authentic sample of $\text{Re}(\text{dmb})(\text{CO})_3(\text{OC}(\text{O})\text{OH})$ prepared using the published procedure²⁵ is in good agreement with our spectrum. Since the stretching frequencies for $\text{Re}(\text{dmb})(\text{CO})_3(\text{CH}_3\text{CN})$ remain almost unchanged for 10 ms under CO_2 , the reaction with CO_2 is slow or unfavorable. Thus, reactions with CO_2 shown in eqs 7a and 7b were not observed in our transient FTIR experiments.

Similar results were obtained with $[\text{Re}(\text{bpy})(\text{CO})_3(\text{CH}_3\text{CN})]^+$ (ν_{CO} at 2040 and 1937 cm^{-1}): $\text{Re}(\text{bpy})(\text{CO})_3(\text{CH}_3\text{CN})$ (ν_{CO} at 2017 and 1902 cm^{-1}) with formation of $[\text{Re}(\text{bpy})(\text{CO})_3(\text{OC}(\text{O})\text{OH})]^-$ (ν_{CO} at 1988 and 1870 cm^{-1}) as a side product. We isolated solids during transient FTIR measurements using $^{12}\text{CO}_2$ and $^{13}\text{CO}_2$ with $[\text{Re}(\text{bpy})(\text{CO})_3(\text{CH}_3\text{CN})]^+$ and confirmed that they are bicarbonate species: IR (KBr) 2021.9, 1895.0, 1617.9 (1578.8), 1602 sh, 1471.5, 1442.9 sh, 1425.3 (1398.8), 1361.2 (1346.5), 1316.3, 1245.4, 1158.6 cm^{-1} . The numbers in parentheses indicate IR shifts due to ^{13}C labeling of the bound $\text{OC}(\text{O})\text{OH}$. ^{13}C was not incorporated into the bound CO.

Properties of Reduced $\text{Re}(\text{dmb})(\text{CO})_3(\text{OTf})$ Species. Thermal formation of rhenium-bicarbonate species makes it difficult to observe any CO_2 -containing intermediates in solutions containing $[\text{Re}(\text{diimine})(\text{CO})_3(\text{CH}_3\text{CN})]^+$, TEA, and CO_2 as discussed above. To avoid complications such as formation of $\text{Re}(\text{dmb})(\text{CO})_3(\text{OC}(\text{O})\text{OH})$ under CO_2 , we generated the one- and two-electron-reduced species of $\text{Re}(\text{dmb})(\text{CO})_3(\text{OTf})$ by Na–Hg reduction in dry solvents. Since the reported reduction potentials for a series of Re complexes have been measured using different solvents, reference electrodes, working electrodes, and scan rates, we reexamined their reduction potentials (vs SCE) using a glassy carbon electrode in CH_3CN solutions containing 0.1 M Bu_4NPF_6 at a scan rate of 100 mV s^{-1} . Before and after each measurement, ferrocene was measured as a standard (0.39 V vs SCE). The results are summarized in Table S1 (Supporting Information). Upon Na–Hg reduction of a yellow THF solution containing $\text{Re}(\text{dmb})(\text{CO})_3(\text{OTf})$, formation of the reddish-purple ligand radical species, $\text{Re}(\text{dmb})(\text{CO})_3(\text{THF})$, with characteristic bands at 356, 467, and 496 nm, was observed. However, within 1 h, $\text{Re}(\text{dmb})(\text{CO})_3(\text{THF})$ converts thermally to a species which has bands at 480, 620, and 818 nm. This change from a reddish-purple solution to a blue-green solution is due to the dimerization of $\text{Re}(\text{dmb})(\text{CO})_3(\text{THF})$ (eq 8). The dimerization has been observed previously in the electrochemical reduction of $\text{Re}(\text{dmb})(\text{CO})_3\text{Cl}$.^{15,22}



Further reduction of $[\text{Re}(\text{dmb})(\text{CO})_3]_2$ produces the five-coordinate $[\text{Re}(\text{dmb})(\text{CO})_3]^-$ species⁴⁷ which has an absorption maximum at 582 nm, similar to $[\text{Re}(\text{bpy})(\text{CO})_3]^-$ reported previously.²³ Similar spectral changes from $\text{Re}(\text{dmb})(\text{CO})_3(\text{OTf})$ to $[\text{Re}(\text{dmb})(\text{CO})_3]^-$ were observed in CH_3CN . The two-electron-reduced species $[\text{Re}(\text{bpy})(\text{CO})_3]^-$ and $[\text{Re}(\text{dmb})(\text{CO})_3]^-$ are quite stable in very dry air-free solvents, especially in THF, despite reports to the contrary.⁴⁸ No decomposition of $[\text{Re}(\text{dmb})(\text{CO})_3]^-$ in THF was observed overnight. The

(47) Our DFT calculations reveal that $[\text{Re}(\text{bpy})(\text{CO})_3(\text{THF})]^-$ is unstable and spontaneously dissociates to the five-coordinate $[\text{Re}(\text{bpy})(\text{CO})_3]^-$. The detailed results will be published in a forthcoming paper (with J. T. Muckerman, BNL).

(48) O'Toole, T. R.; Younathan, J. N.; Sullivan, B. P.; Meyer, T. J. *Inorg. Chem.* **1989**, *28*, 3923–3926.

(46) Unpublished data (K. Shinozaki, Yokohama City University, Japan).

Table 2. Spectroscopic Properties of Re(dmb)(CO)₃(OTf) and the Reduced Species at 25 °C

spectroscopy	complexes	solvent		
UV–vis ^a	Re(dmb)(CO) ₃ (OTf)	THF	248 (17.0), 306 (11.6), 318 (11.5), 346 (4.4)	
		THF	356, 467, 496	
	Re(dmb)(CO) ₃ S	CH ₃ CN	400, 482, 508	
		DMF	490, 520	
	[Re(dmb)(CO) ₃] ₂	THF	480 (8.1), 520sh (7.2), 620 (5.6), 818 (17.6)	
		CH ₃ CN	438 (7.7), 598 (7.8), 780 (6.8)	
		acetone	454, 606, 798	
	[Re(dmb)(CO) ₃] [–]	THF	282 (24.5), 378sh (8.8), 582 (13.1)	
		CH ₃ CN	582 (10.2)	
	IR ^b	Re(dmb)(CO) ₃ (OTf)	THF	2032, 1932, 1908
			DMF	2028, 1915(br)
		Re(dmb)(CO) ₃ S	THF ^c	2007, 1897(br)
CH ₃ CN			2012, 1904(br)	
[Re(dmb)(CO) ₃] ₂		THF	1976, 1947, 1877, 1855	
		DMF	1978, 1942, 1879, 1840	
		CH ₃ CN	1982, 1943, 1876, 1843	
[Re(dmb)(CO) ₃] [–]		THF	1940, 1832	
		CH ₃ CN	1943, 1828	
NMR ^d		Re(dmb)(CO) ₃ (OTf)	THF	8.93(d), 8.39(s), 7.54(d), 2.58(s)
			DMF	9.07(d), 8.39(s), 7.79(d), 2.65(s)
		[Re(dmb)(CO) ₃] ₂	DMF	8.25(s), 7.96(d), 7.05(d), 2.61(s)
	THF		8.87(d), 7.08(s), 5.18(d), 2.07(s)	
	[Re(dmb)(CO) ₃] [–]	THF	8.93(d), 8.39(s), 7.54(d), 2.58(s)	
		DMF	9.07(d), 8.39(s), 7.79(d), 2.65(s)	

^a λ_{max}, nm, (ε, mM^{–1} cm^{–1}), ^b ν_{CO}, cm^{–1}, ^c Unpublished data (K. Shinozaki), ^d Chemical shift, ppm

Table 3. Spectroscopic Properties of C-Containing Products from the Reaction of Re(dmb)(CO)₃ with CO₂ or Other Reactions at 25 °C

spectroscopy	complexes	solvent		
UV–vis ^a	Re(dmb)(CO) ₃ (COOH)	DMF	290sh (13.9), 316sh (6.6), 374(3.1)	
	Re(dmb)(CO) ₃ (OCHO)	DMF	288 (12.8), 316sh (8.5), 360 (3.4)	
	[Re(dmb)(CO) ₃] ₂ (CO ₂)	DMF	290 (25.2), 362 (4.4), 460 (2.5)	
	Re(dmb)(CO) ₃ (OC(O)OH)	DMF	288(11.3), 316 (7.1), 360 (2.8)	
	Re(dmb)(CO) ₃ (COOH)	DMF	2005, 1895	
IR ^b	Re(dmb)(CO) ₃ (OCHO)	KBr	2008, 1886, 1620(ν _{dmb}), 1592(ν _{COOH}), 1194(ν _{COOH}),	
		DMF	2017, 1911, 1888	
	[Re(dmb)(CO) ₃] ₂ (CO ₂)	DMF	2002, 1989, 1896, 1867	
		KBr	2000, 1993, 1889, 1869, 1620(ν _{dmb}), 1486(ν _{COO}), 1176(ν _{COO})	
	[Re(dmb)(CO) ₃] ₂ (O ¹² C ₂)	DMF	2011, 1899, 1871	
		KBr	2019, 1894, 1869, 1853, 1621(ν _{dmb}), 1576(ν _{OCO2}), 1288(ν _{OCO2}), 1269(ν _{OCO2})	
	[Re(dmb)(CO) ₃] ₂ (O ¹³ C ₂)	KBr	2019, 1894, 1869, 1853, 1621(ν _{dmb}), 1534(ν _{OCO2}), 1262(ν _{OCO2}), 1238(ν _{OCO2})	
		DMF	2017, 1912, 1886	
	Re(dmb)(CO) ₃ (O ¹³ C(O)OH)	KBr	2020, 1905, 1869, 1620(ν _{dmb}), 1620(ν _{OCO}), 1416(ν _{OCO}), 1353(ν _{OCO})	
		KBr	2020, 1905, 1869, 1620(ν _{dmb}), 1584(ν _{OCO}), 1384(ν _{OCO}), 1331(ν _{OCO})	
	Re(dmb)(CO) ₃ Cl	DMF	2018, 1911, 1890, 1623(ν _{dmb})	
		KBr	2020, 1895(br), 1605(ν _{bpy}), 1617(ν _{OCO}), 1425(ν _{OCO}), 1361(ν _{OCO})	
	Re(bpy)(CO) ₃ (O ¹² C(O)OH)	KBr	2020, 1895(br), 1605(ν _{bpy}), 1579(ν _{OCO}), 1399(ν _{OCO}), 1346(ν _{OCO})	
		DMF	2021, 1892(br), 1602(ν _{bpy})	
	¹³ C NMR	Re(dmb)(CO) ₃ (OCHO)	DMF	199.6, 195.8, 167.0(HOCO)
		[Re(dmb)(CO) ₃] ₂ (CO ₂)	DMF	212.2(CO ₂), 203.7, 202.3, 200.7, 196.5
		[Re(dmb)(CO) ₃] ₂ (OCO ₂)	DMF	200.7, 196.8, 166.7(OCO ₂)
		Re(dmb)(CO) ₃ (OC(O)OH)	DMF	199.7, 196.0, 160.4(OCO ₂ H)
¹ H NMR ^c	Re(dmb)(CO) ₃ (COOH)	DMF	9.07(bs, COOH), 8.93 (d), 8.67 (s), 7.56 (d), 2.59 (s)	
		THF	8.93(d), 8.39(s), 7.54(d), 2.58(s)	
	Re(dmb)(CO) ₃ (OCHO)	DMF	9.00(d), 8.72(s), 7.88(s, OCHO), 7.67(d), 2.62(s)	
		DMF	8.62(d), 8.49(d), 8.47(s), 8.27(s), 7.42(d), 7.26(d), 2.66(s), 2.59(s)	
	[Re(dmb)(CO) ₃] ₂ (OCO ₂)	DMF	8.75–8.68(d), 8.37–8.03(s), 7.46–7.26(d), 2.42–2.10(s)	
		DMF	9.21(bs, OC(O)OH), 8.99(d), 8.69(s), 7.66(d), 2.60(s)	

^a λ_{max}, nm (ε, mM^{–1} cm^{–1}), ^b ν_{CO} unless mentioned, cm^{–1}, ^c Chemical shift, ppm.

UV–vis spectra of Re(dmb)(CO)₃(OTf), [Re(dmb)(CO)₃]₂, and [Re(dmb)(CO)₃][–] are shown in Figure S1 (Supporting Information). The UV–vis, IR, and NMR data are summarized in Tables 2 and 3. Note that while UV–vis spectra of [Re(dmb)(CO)₃]₂ are solvent dependent probably due to the charge-transfer origin of the absorption, those of [Re(dmb)(CO)₃][–] in CH₃CN and THF are remarkably similar.

The IR spectra of Re(dmb)(CO)₃S, [Re(dmb)(CO)₃]₂, and their bpy analogues are controversial: Re(dmb)(CO)₃S 1979, 1876, and 1843 cm^{–1} in CH₃CN by Christensen et al.;²² [Re(dmb)(CO)₃]₂ 1943 cm^{–1} in CH₃CN by Christensen et al.;²²

[Re(bpy)(CO)₃]₂ (KBr) 2020, 1940, and 1860 cm^{–1} by Hawecker et al.;⁵ [Re(bpy)(CO)₃]₂ in CH₃CN 1975 cm^{–1} by O'Toole et al.;¹⁶ [Re(bpy)(CO)₃]₂ in THF 1988, 1951, 1887, and 1859 cm^{–1} by Stor et al.²³ We believe that all these assignments, except that of Stor et al., are probably due to contamination by oxidized or further reduced species and complicated further by the monomer/dimer equilibrium (See Table 2 for our data in THF, DMF, and CH₃CN). Note that protons for [Re(dmb)(CO)₃]₂ and [Re(dmb)(CO)₃][–] show a significant high field shift in their NMR spectra. Sharp methyl and C₅ proton signals of [Re(dmb)(CO)₃][–] at 2.07 (s) and 5.18 (d) ppm, respectively,

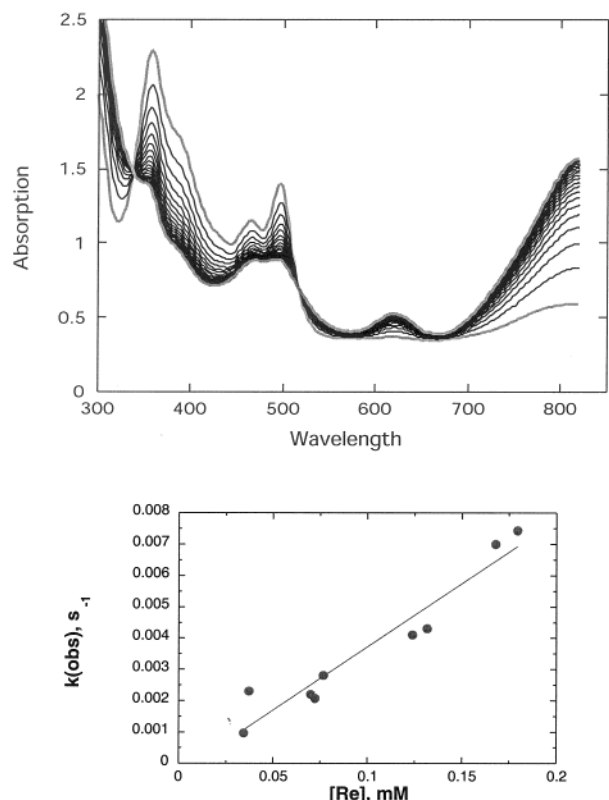


Figure 2. (Top) Dimerization of $\text{Re}(\text{dmb})(\text{CO})_3(\text{THF})$ in THF: spectral changes of a solution containing 0.10 mM $[\text{Re}(\text{dmb})(\text{CO})_3]_2$ monitored every 60 s after photolysis (>380 nm). (Bottom) Plot of observed pseudo-first-order rate constant for dimerization of $\text{Re}(\text{dmb})(\text{CO})_3(\text{THF})$ in THF at 25 °C vs $[\text{Re}(\text{dmb})(\text{CO})_3(\text{THF})]$ concentration.

are strikingly shifted from those of $\text{Re}(\text{dmb})(\text{CO})_3(\text{OTf})$ at 2.58 and 7.54 ppm.

Photochemistry of $[\text{Re}(\text{dmb})(\text{CO})_3]_2$. Dark blue-green solid $[\text{Re}(\text{dmb})(\text{CO})_3]_2$ was prepared by sodium amalgam (Na–Hg) reduction of $\text{Re}(\text{dmb})(\text{CO})_3(\text{OTf})$ in THF. The UV–vis spectra show solvent dependence: λ_{max} (ϵ , $\text{M}^{-1} \text{cm}^{-1}$); 480 (8100), 520sh (7200), 620 (5600), and 818 (17600) nm in THF; 454, 606, and 798 nm in acetone; 438 (7700), 598 (7800), and 780 (6800) nm in acetonitrile (Figure S2 in the Supporting Information). The spectrum in CH_3CN is consistent with those published previously.^{15,49} Polar solvents cause a shift of the visible transitions of the dimer to higher energy indicating that these absorptions can be assigned to MLCT transitions. There is no other absorption band in the near-IR region (900–1600 nm).

Upon photolysis ($\lambda > 380$ nm) of a THF solution containing 0.1 mM $[\text{Re}(\text{dmb})(\text{CO})_3]_2$, Re–Re bond homolysis takes place to form the $\text{Re}(\text{dmb})(\text{CO})_3(\text{THF})$ monomer, which is a ligand radical with characteristic absorptions at 467 and 496 nm (eq 9). The homolysis quantum yield is quite small ($\sim 10^{-5}$ at 530 nm). As shown in Figure 2 (top), the monomer reversibly reforms the dimer after photolysis at 25 °C. Formation of the dimer is surprisingly slow and is second order in $[\text{Re}(\text{dmb})(\text{CO})_3(\text{THF})]$ with $k_{\text{d}} = 40 \pm 5 \text{ M}^{-1} \text{ s}^{-1}$ (eq 9) at 25 °C in THF as seen in Figure 2 (bottom). The homolysis/dimerization process for $[\text{Re}(\text{dmb})(\text{CO})_3]_2$ was also observed in CH_3CN and

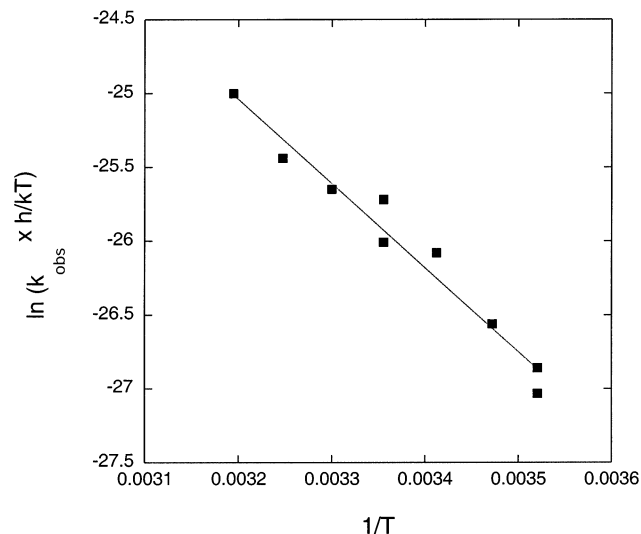
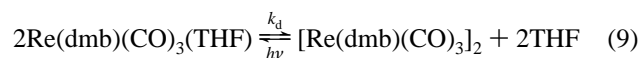


Figure 3. Eyring plot of $\ln(k_{\text{obs}} \times h/kT)$ vs $1/T$ for the dimerization reaction of $\text{Re}(\text{dmb})(\text{CO})_3(\text{THF})$. The rate constants of the dimerization (k_{obs}) were measured at 11, 15, 20, 25, 30, 35, and 40 °C. Activation entropy ($\Delta H^\ddagger = 11 \text{ kcal mol}^{-1}$) and enthalpy ($\Delta S^\ddagger = -14 \text{ cal mol}^{-1} \text{ deg}^{-1}$) are calculated from the slope and the intercept, respectively.

DMF on a similar time scale; however, it was not completely reversible. Only $1/2$ to $2/3$ of the original $[\text{Re}(\text{dmb})(\text{CO})_3]_2$ was recovered after homolysis. CW photolysis ($\lambda > 380$ nm) of 3 mM $[\text{Re}(\text{dmb})(\text{CO})_3]_2$ for 2 h in DMF under Ar (no added CO_2) surprisingly yields $\text{Re}(\text{dmb})(\text{CO})_3(\text{OC}(\text{O})\text{OH})$ ($\sim 30\%$) with no CO generation. $\text{Re}(\text{dmb})(\text{CO})_3(\text{OC}(\text{O})\text{OH})$ seems to form from CO_2 produced by the photodecomposition of impurities or solvent.



$$k_{\text{obs}} = \frac{k_{\text{B}}T}{h} \exp(-\Delta H^\ddagger/RT) \exp(\Delta S^\ddagger/R) \quad (10)$$

Activation parameters (eq 10) for the dimerization reaction (eq 9) of $\text{Re}(\text{dmb})(\text{CO})_3(\text{THF})$ in THF are $\Delta H^\ddagger = 11 \text{ kcal mol}^{-1}$ and $\Delta S^\ddagger = -14 \text{ cal mol}^{-1} \text{ deg}^{-1}$ (See Figure 3). Flash photolysis studies of compounds containing the M–M bond shows that visible excitation induces homolysis of the M–M bond with formation of $17e^-$ metal radicals such as $\text{Re}^*(\text{CO})_5$ ^{50,51} and $\text{CpM}^*(\text{CO})_3$,^{52,53} which then dimerize to reform the parent species with a rate constant of $10^9 \text{ M}^{-1} \text{ s}^{-1}$ in solvents such as cyclohexane, CH_3CN , and THF. In our case, the species formed by the homolysis is not a $17e^-$ metal radical but rather an $18e^-$ six-coordinate $\text{Re}(\text{dmb})(\text{CO})_3(\text{THF})$ with a dmb anion radical. If the dimerization reaction that we observe proceeds via a preequilibrium to the metal-centered radical, eq 11, then the unfavorable preequilibrium is the dominant barrier to the reaction. Reaction 12 proceeds rapidly due to the unstable nature of the six-coordinate $19e^-$ species. Provided $\Delta S_{11} \approx 0$, the

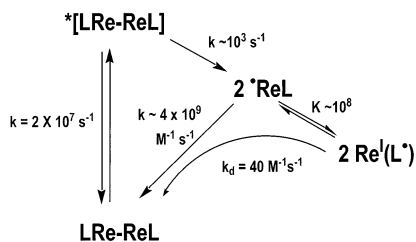
(50) Meckstroth, W. K.; Walters, R. T.; Waltz, W. L.; Wojcicki, A.; Dorfman, L. M. *J. Am. Chem. Soc.* **1982**, *104*, 1842–1846.

(51) Wegman, R. W.; Olsen, R. J.; Gard, D. R.; Faulkner, L. R.; Brown, T. L. *J. Am. Chem. Soc.* **1981**, *103*, 6089–6092.

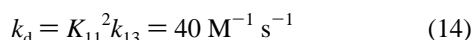
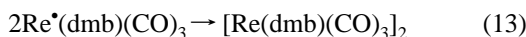
(52) Meyer, T. J.; Caspar, J. V. *Chem. Rev.* **1985**, *85*, 187–218.

(53) Scott, S. L.; Espenson, J. H.; Zhu, Z. *J. Am. Chem. Soc.* **1993**, *115*, 1789–1797.

(49) O'Toole, T. R.; Sullivan, B. P.; Meyer, T. J. *J. Am. Chem. Soc.* **1989**, *111*, 5699–5706.

Scheme 2. Photolysis of $[\text{Re}(\text{dmb})(\text{CO})_3]_2$ and Recombination of the Radicals

equilibrium constant (K_{11}) may be estimated from $\Delta H_{11} \approx \Delta H^\ddagger/2$, $K_{11} \approx \exp(-\Delta H^\ddagger/2RT) = 10^{-4}$.



Thus, the extremely slow dimerization of $\text{Re}(\text{dmb})(\text{CO})_3(\text{THF})$ may arise from unfavorable equilibrium K_{11} (eq 11). Assuming eq 14, then the dimerization rate constant (k_{13}) by the metal radical (eq 13) is $\approx 4 \times 10^9 \text{ M}^{-1} \text{ s}^{-1}$, consistent with other metal $17e^-$ systems (Scheme 2).

Flash photolysis experiments on $[\text{Re}(\text{dmb})(\text{CO})_3]_2$ in THF were carried out using excitation with the second or third harmonic of an Nd:YAG laser. We did not see formation of a long-lived $\text{Re}(\text{dmb})(\text{CO})_3(\text{THF})$ monomer, consistent with the low quantum yield of the homolysis determined in the CW photolysis. Figure 4 shows the transient absorption spectrum of a short-lived species observed after excitation of a degassed sample containing 0.07 mM $[\text{Re}(\text{dmb})(\text{CO})_3]_2$ in THF at 15 °C. The decay of the signal is first order with $k_{\text{obs}} = 2.1 \times 10^7 \text{ s}^{-1}$. An experiment under 1 atm of CO gave identical results, indicating that CO dissociation does not occur on the nanosecond to millisecond time scale. The transient spectrum does not resemble that of $[\text{Re}(\text{dmb})(\text{CO})_3]^-$; therefore, heterolysis to form $[\text{Re}(\text{dmb})(\text{CO})_3]^+$ and $[\text{Re}(\text{dmb})(\text{CO})_3]^-$ does not take place at this time scale.

Morse and Wrighton⁵⁴ have assigned the lowest energy absorption in $(\text{phen})(\text{CO})_3\text{Re}-\text{Re}(\text{CO})_5$ to a $\sigma_{\text{MM}} \rightarrow \pi^*_{\text{phen}}$ charge-transfer transition that transfers charge from the metal–metal bonding orbital (d_z^2 orbital on the Re centers) to an antibonding orbital on the phen ligand. The transition is observed to be solvent sensitive (572 nm in isoctane, 541 nm in benzene, 578 nm in CH_2Cl_2 , and 500 nm in acetone). The $d\pi_{\text{MM}} \rightarrow \pi^*_{\text{phen}}$ transition, normally indicated as the MLCT transition, occurs at higher energy. The initially formed ^1CT state ($^1\sigma_{\text{MM}}-\pi^*_{\text{phen}}$) internally converts to the ^3CT ($^3\sigma_{\text{MM}}-\pi^*_{\text{phen}}$). Homolytic bond cleavage of the Re–Re bond then takes place. The quantum yield of ~ 0.17 is independent of the excitation wavelength from 313 to 633 nm at 25 °C. Morse et al. postulated that the depopulation of the σ_{MM} -orbital causes the Re–Re bond to break. Meyer and Caspar,⁵² however, argued that the initially formed ^1CT state rapidly undergoes internal conversion to the nonbonding $^3\sigma_{\text{MM}}-\sigma_{\text{MM}}^*$ state, which leads to rapid homolysis of the Re–Re bond. Stufkens^{55,56} later pointed out that the

(54) Morse, D. L.; Wrighton, M. S. *J. Am. Chem. Soc.* **1976**, *98*, 3931–3934.

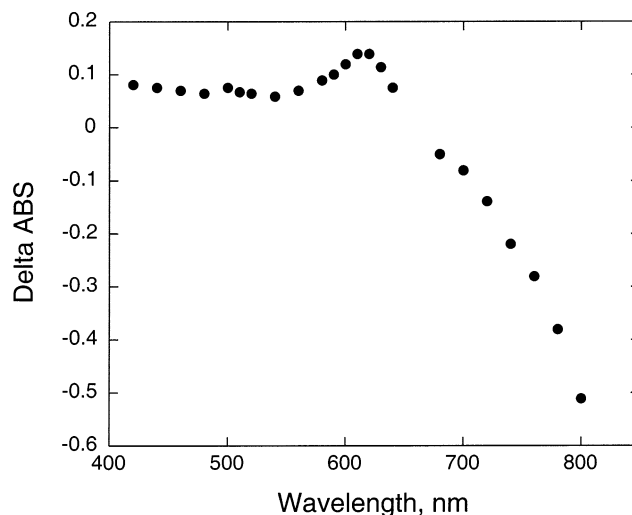


Figure 4. Transient absorption spectrum of a short-lived excited-state species observed after excitation (532 nm) of a degassed sample containing 0.07 mM $[\text{Re}(\text{dmb})(\text{CO})_3]_2$ in THF at 15 °C.

assignment of the lowest-energy absorption of metal–metal bonded complexes may be a mixture of $\sigma_{\text{MM}} \rightarrow \pi^*_{\text{phen}}$ and $d\pi_{\text{MM}} \rightarrow \pi^*_{\text{phen}}$ due to the similar energies of the σ_{MM} - and the $d\pi_{\text{MM}}$ -orbitals.^{57,58} Rapid internal conversion after excitation yields the $^3\sigma_{\text{MM}}-\pi^*_{\text{phen}}$ CT state. Stufkens^{57,58} attributes the photochemistry to this state. Small changes in the relative energies of the various orbitals are expected to lead to significant changes in the photochemistry and photophysics of the Re–Re dimers. If the reactive state is the $^3\sigma_{\text{MM}}-\sigma_{\text{MM}}^*$ state and the surface crossing from the $^3\sigma_{\text{MM}}-\pi^*_{\text{phen}}$ state is energetically unfavorable, only a small fraction of the excited molecules will cross to the $^3\sigma_{\text{MM}}-\sigma_{\text{MM}}^*$ state (Figure 5). However, if the crossing becomes barrierless, then the fraction would approach unity. To understand the photophysics and photochemistry of $[\text{Re}(\text{dmb})(\text{CO})_3]_2$, B3LYP hybrid DFT and fully ab initio RHF/MP2 calculations on $[\text{Re}(\text{dmb})(\text{CO})_3]_2$ and the homolysis product are currently under investigation.⁵⁹

Reaction of $\text{Re}(\text{dmb})(\text{CO})_3\text{S}$ with CO_2 . $[\text{Re}(\text{dmb})(\text{CO})_3]_2$ does not react with CO_2 without irradiation. When a THF solution containing 0.05 mM $[\text{Re}(\text{dmb})(\text{CO})_3]_2$ and 0.8 atm of CO_2 was photolyzed by a 150 W Xe lamp with a 380 nm low pass filter for 20 s, only 45% of the $[\text{Re}(\text{dmb})(\text{CO})_3]_2$ was recovered. The rest of $\text{Re}(\text{dmb})(\text{CO})_3(\text{THF})$ reacts with CO_2 , and the observed rate is $\sim 0.003 \text{ s}^{-1}$. Thus, CO_2 binding of $\text{Re}(\text{dmb})(\text{CO})_3\text{S}$ competes with dimerization. Since the product of CO_2 binding undergoes photodecomposition (see next section), further kinetic study of CO_2 binding to $\text{Re}(\text{dmb})(\text{CO})_3\text{S}$ was not carried out in THF.

Sullivan et al. reported their preliminary study of photolysis of $[\text{Re}(\text{bpy})(\text{CO})_3]_2$ in CO_2 -saturated DMSO to yield some CO and $\text{Re}(\text{bpy})(\text{CO})_3(\text{OCO}_2\text{H})$.¹⁴ They proposed that the photochemical reaction involves initial Re–Re bond cleavage, followed by entry of the monomers into the CO_2 reduction cycle. To identify intermediates in the reaction of $\text{Re}(\text{dmb})(\text{CO})_3\text{S}$ with $^{13}\text{CO}_2$, a DMF suspension containing 3–16 mM $[\text{Re}(\text{dmb})-$

(55) Stufkens, D. J. *Comments Inorg. Chem.* **1992**, *13*, 359–385.

(56) Stufkens, D. J.; Vlcek, A. *Coord. Chem. Rev.* **1998**, *177*, 127–179.

(57) Kokkes, M. W.; Snoeck, T. L.; Stufkens, D. J.; Oksam, A.; Christophersen, M.; Stam, C. H. *J. Mol. Struct.* **1985**, *131*, 11.

(58) Larson, L. J.; Oksam, A.; Zink, J. I. *Inorg. Chem.* **1991**, *30*, 42.

(59) The detailed results will be published in a forthcoming paper (with J. T. Muckerman, BNL).

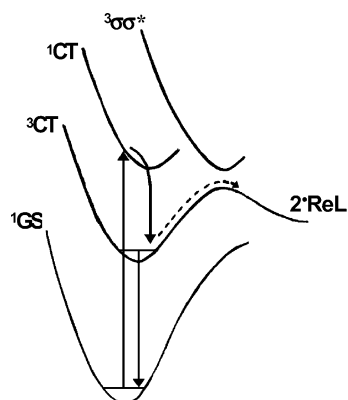
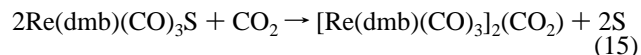


Figure 5. Schematic potential energy-coordinate diagram for photolysis of $[\text{Re}(\text{dmb})(\text{CO})_3]_2$.

$(\text{CO})_3]_2$ was monitored by ^1H NMR, ^{13}C NMR, FTIR, and GC. The ^1H NMR spectrum after a 2 min photolysis is shown in Figure 6 along with the ^{13}C NMR spectrum (insert). A carboxylate-bridged Re dimer $[\text{Re}(\text{dmb})(\text{CO})_3]_2(\text{CO}_2)$ appears at δ 8.63 (2H, d), 8.49 (2H, d), 8.47 (2H, s), 8.26 (2H, s), 7.42 (2H, d), and 7.26 (2H, d), together with the starting material, $[\text{Re}(\text{dmb})(\text{CO})_3]_2$, at δ 8.24 (2H, s), 7.96 (2H, d), and 7.04 (2H, d) as shown in Figure 6, Table 3, and eq 15. Furthermore, a carbonate-bridged Re dimer $[\text{Re}(\text{dmb})(\text{CO})_3]_2(\text{OCO}_2)$ was observed at δ 8.69 (4H, d), 8.06 (4H, s), and 7.28 (4H, d), overlapping with signals of $\text{Re}(\text{dmb})(\text{CO})_3(\text{OC}(\text{O})\text{OH})$ and $[\text{Re}(\text{dmb})(\text{CO})_3]_2(\text{CO}_2)$. A ^{13}C NMR spectrum of the same solution shows three signals at δ 212.1, 166.7, and 160.4, which are assigned to $[\text{Re}(\text{dmb})(\text{CO})_3]_2(^{13}\text{CO}_2)$, $[\text{Re}(\text{dmb})(\text{CO})_3]_2(\text{O}^{13}\text{CO}_2)$, and $\text{Re}(\text{dmb})(\text{CO})_3(\text{O}^{13}\text{C}(\text{O})\text{OH})$, respectively. In addition, there is a small signal at δ 185.4 that is due to ^{13}CO produced. The above assignments of $[\text{Re}(\text{dmb})(\text{CO})_3]_2(\text{OCO}_2)$

and $\text{Re}(\text{dmb})(\text{CO})_3(\text{OC}(\text{O})\text{OH})$ were consistent with those reported previously.^{24,25}



When the NMR tube containing the above mixture was further irradiated, $[\text{Re}(\text{dmb})(\text{CO})_3]_2$ and $[\text{Re}(\text{dmb})(\text{CO})_3]_2(\text{CO}_2)$ were completely converted to $\text{Re}(\text{dmb})(\text{CO})_3(\text{OC}(\text{O})\text{OH})$ and $[\text{Re}(\text{dmb})(\text{CO})_3]_2(\text{OCO}_2)$ with generation of CO in 25–50% yield based on [Re]. The CO yield increases with Re concentration consistent with a highly reactive nature of the $\text{Re}(\text{dmb})(\text{CO})_3(\text{DMF})$ species that can react with a trace amount of impurities in DMF. H_2 was not detected. The total yield of $\text{Re}(\text{dmb})(\text{CO})_3(\text{OC}(\text{O})\text{OH})$ and $[\text{Re}(\text{dmb})(\text{CO})_3]_2(\text{OCO}_2)$ was 60–100% based on [Re]. The ratio between both the two final products, $\text{Re}(\text{dmb})(\text{CO})_3(\text{OC}(\text{O})\text{OH})$ and $[\text{Re}(\text{dmb})(\text{CO})_3]_2(\text{OCO}_2)$, depends on Re and H_2O concentrations. An increase in the concentration of $[\text{Re}(\text{dmb})(\text{CO})_3]_2$ increases the yield of $[\text{Re}(\text{dmb})(\text{CO})_3]_2(\text{OCO}_2)$. Furthermore, on standing, $\text{Re}(\text{dmb})(\text{CO})_3(\text{OC}(\text{O})\text{OH})$ gradually converts to $[\text{Re}(\text{dmb})(\text{CO})_3]_2(\text{OCO}_2)$, which precipitates. Although Hawecker et al.⁵ reported formation of the formate complex $\text{Re}(\text{bpy})(\text{CO})_3(\text{OCHO})$ in their photocatalytic CO_2 reduction with $\text{Re}(\text{bpy})(\text{CO})_3\text{Cl}$, we did not observe any formation of $\text{Re}(\text{dmb})(\text{CO})_3(\text{OCHO})$ in our system. The difference may arise from use of TEOA as an electron donor in their system. Interestingly, they did not report formation of $\text{Re}(\text{bpy})(\text{CO})_3(\text{OC}(\text{O})\text{OH})$ or $[\text{Re}(\text{bpy})(\text{CO})_3]_2(\text{OCO}_2)$ complexes. Furthermore, while incorporation of ^{13}CO to the rhenium complexes was reported,⁵ we did not observe any enhancement of the bound ^{13}CO signals. The predicted mononuclear CO_2 adduct,¹⁴ $\text{Re}(\text{dmb})(\text{CO})_3(\text{CO}_2)$ in eq 6, has not been observed in our experiments. $\text{Re}(\text{dmb})(\text{CO})_3(\text{COOH})$ was observed as a minor product only when wet DMF was used as a solvent in NMR experiments.

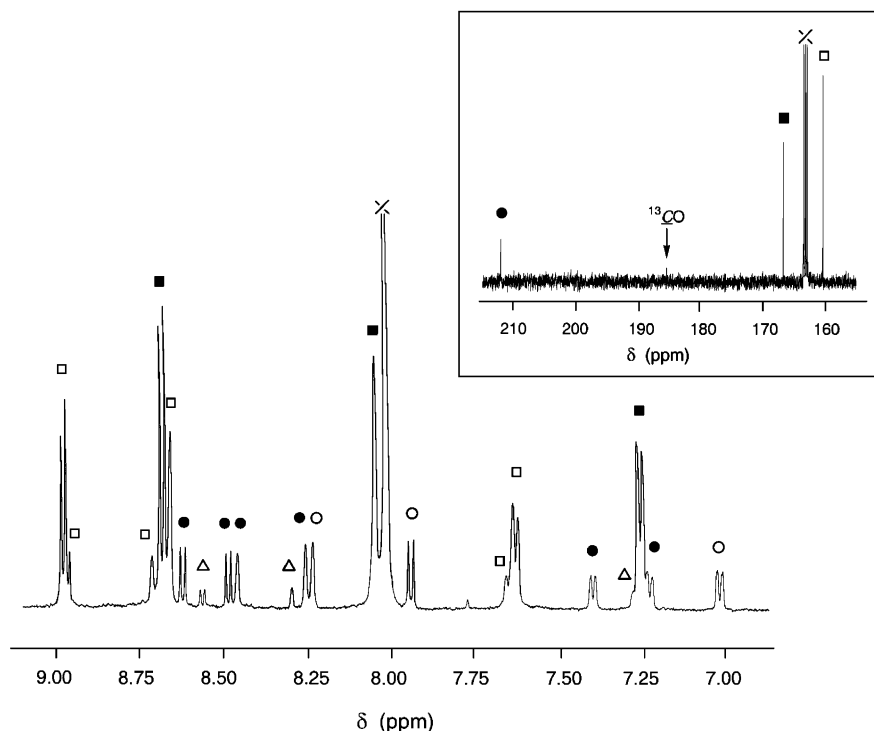


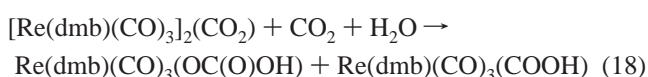
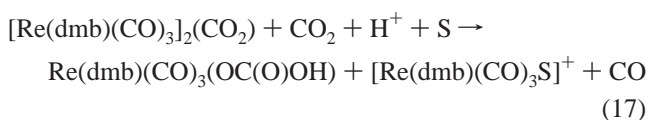
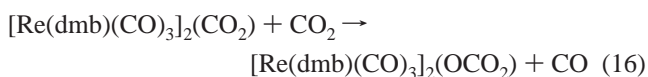
Figure 6. ^1H NMR spectrum of reaction products of $\text{Re}(\text{dmb})(\text{CO})_3(\text{DMF})$ with CO_2 in d_7 -DMF: (●) $[\text{Re}(\text{dmb})(\text{CO})_3]_2(\text{CO}_2)$, (■) $[\text{Re}(\text{dmb})(\text{CO})_3]_2(\text{OCO}_2)$, (○) $[\text{Re}(\text{dmb})(\text{CO})_3]_2$, (□) $\text{Re}(\text{dmb})(\text{CO})_3(\text{OC}(\text{O})\text{OH})$, and (△) dmb .

Christensen et al. reported²² an in situ IR study of electrochemical reduction of Re(dmb)(CO)₃Cl in CH₃CN in the presence of CO₂. They concluded that direct attack of CO₂ on Re(dmb)(CO)₃Cl led to formation of Re(dmb)(CO)₃(COOH) (ν_{CO} : 2010, 1902, and 1878 cm⁻¹), which can undergo further reduction to [Re(dmb)(CO)₃(COOH)]⁻ (ν_{CO} : 1997 and 1860 cm⁻¹), in the absence of water. Their assignment of Re(dmb)(CO)₃(COOH) in their experiments is not consistent with either our data (in DMF: 2005, 1895 cm⁻¹; KBr: 2008, 1886 cm⁻¹) or the data by Gibson et al.²⁴ (DRIFT, KCl: 2012, 1916 sh, 1892 cm⁻¹). We did not observe the formation of Re(dmb)(CO)₃(COOH) as a major product in our IR and NMR study in DMF. It is very difficult to identify the species produced during bulk electrolysis only from ν_{CO} . For example, we note that IR (ν_{CO}) spectra of Re(dmb)(CO)₃(OCHO), Re(dmb)(CO)₃(OC(O)OH), and Re(dmb)(CO)₃Cl are almost identical in DMF. Considering the fact that loss of Cl⁻ from [Re(dmb)(CO)₃Cl]⁻ is slow and that reaction of CO₂ with the one-electron-reduced species is very slow, we believe it is possible that no CO₂-containing species coexist in their solution at the applied potential used.

Reactions of [Re(dmb)(CO)₃]₂(CO₂). The reactivity of [Re(dmb)(CO)₃]₂(CO₂), prepared by the reaction of Re(dmb)(CO)₃COOH with Re(dmb)(CO)₃OH,²⁴ was monitored in DMF by NMR, IR, and UV–vis spectroscopy. [Re(dmb)(CO)₃]₂(CO₂) is stable in DMF at ambient temperature in the absence of CO₂: a 1mM solution of [Re(dmb)(CO)₃]₂(CO₂) in *d*₇-DMF decomposes very slowly under Ar to Re(CO)₃(OC(O)OH) in 30% yield based on [Re] along with [Re(dmb)(CO)₃S]⁺ (5%) and free dmb (11%) over a 6 month period.

Gibson et al. reported that, under CO₂ atmosphere, [Re(dmb)(CO)₃]₂(CO₂) is readily converted to Re(dmb)(CO)₃OC(O)OH in wet DMF or DMSO.²⁵ The formation of CO was not described in their paper. Our NMR experiments using a *d*₇-DMF suspension of [Re(dmb)(CO)₃]₂(CO₂) with ¹³C₂O₂ showed the formation of Re(dmb)(CO)₃(OC(O)OH) and [Re(dmb)(CO)₃]₂(OCO₂) with a combined yield of ≈90% and CO ≈45% based on [Re] in a few hours.

To obtain detailed insight into the reactivity of [Re(dmb)(CO)₃]₂(CO₂) with CO₂ in DMF, the decay of a 1.8 × 10⁻⁴ M [Re(dmb)(CO)₃]₂(CO₂) solution was monitored as a function of CO₂ (0.1–0.2 M) at 25 °C by UV–vis spectroscopy. The CO₂ solubility, [CO₂] = 0.197 M under 1 atm of CO₂, was taken from published data.⁶⁰ The disappearance of [Re(dmb)(CO)₃]₂(CO₂) is first order in [CO₂]. The bimolecular rate constant, *k*₁₆, is 9.7 × 10⁻⁴ M⁻¹ s⁻¹ (Figure S3), consistent with eq 16.

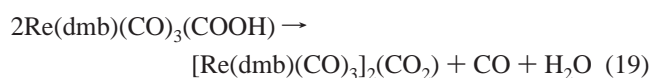


If H₂O is present, formation of Re(dmb)(CO)₃(OC(O)OH) is possible (eqs 17 and 18). Unfortunately studies with small amounts of added water did not yield consistent results for reactions 16–18.

While the above thermal reactions took place in a few hours, the CW photolysis of 5–6 mM [Re(dmb)(CO)₃]₂(CO₂) under CO₂ produces [Re(dmb)(CO)₃]₂(OCO₂) (and Re(dmb)(CO)₃(OC(O)OH)) in a few minutes along with CO (23–43% yield based on [Re]). The decay of a 1.9 × 10⁻⁴ M [Re(dmb)(CO)₃]₂(CO₂) solution was monitored as a function of CO₂ (0.07–0.2 M) at 25 ± 2 °C under irradiation ($\lambda > 380$ nm, 150 W Xe lamp). The bimolecular rate constant under irradiation is 5.1 × 10⁻² M⁻¹ s⁻¹ (Figure S4), which is about 50 times larger than that of the thermal reaction. Although the photoinduced reaction should be dependent on light-intensity, excitation wavelength, sensitizer/catalyst concentration, and so forth, our results show at least that the reported⁵ turnover frequency of photochemical CO generation of ~8 hr⁻¹ is feasible with a [Re(dmb)(CO)₃]₂(CO₂) intermediate. Photolysis (<5min) of [Re(dmb)(CO)₃]₂(CO₂) under Ar produces [Re(dmb)(CO)₃]₂ as the main product in 11–15% yield based on [Re] with a small amount of two unknown species. No CO generation was observed, indicating that CO was not released simply from [Re(dmb)(CO)₃]₂(CO₂) upon photolysis.

Roles of Re(dmb)(CO)₃(COOH) and Re(dmb)₃(CO)(CHO) in Photochemical CO₂. Gibson et al. prepared Re(dmb)(CO)₃(COOH) by the reaction of Re(dmb)(CO)₄(OTf) with aqueous KOH.²⁴ They reported that the μ_2 - η^2 -CO₂-bridged complex, [Re(dmb)(CO)₃]₂(CO₂), was produced from an acetone, DMF, or DMSO solution of Re(dmb)(CO)₃(COOH) on standing under room light. Although the formation of [Re(dmb)(CO)₃]₂(CO₂) was attributed to partial decarboxylation of Re(dmb)(CO)₃(COOH) to Re(dmb)(CO)₃(H) followed by reaction with another molecule of Re(dmb)(CO)₃(COOH) and liberation of H₂ (and presumably CO₂),²⁴ their recent publication indicates that no H₂ is detected by GC.²¹

We observed Re(dmb)(CO)₃(COOH) as a very minor product together with [Re(dmb)(CO)₃]₂(CO₂), [Re(dmb)(CO)₃]₂(OCO₂), and Re(dmb)(CO)₃(OC(O)OH) in the reaction of Re(dmb)(CO)₃(DMF) with CO₂ only when DMF was slightly wet (0.1 wt % of H₂O added). Therefore, we investigated the reactivity of Re(dmb)(CO)₃(COOH) in DMF. The reaction of 6 mM Re(dmb)(CO)₃(COOH) in *d*₇-DMF under Ar was monitored by ¹H NMR. The solution was kept in the dark at 5 °C except during NMR measurements. With a loss of Re(dmb)(CO)₃(COOH), an increase of [Re(dmb)(CO)₃]₂(CO₂) and water was observed. The final products and yields in this experiment were [Re(dmb)(CO)₃]₂CO₂ (60%), Re(dmb)(CO)₃(OC(O)OH) (30%), CO (66%), and H₂O (80%) based on [Re] (Figure S5, Supporting Information). No H₂ was observed by ¹H NMR or GC, consistent with Gibson's recent results²¹ and eq 19.



Thermal decomposition of metalcarboxylic acids to form μ_2 - η^2 -CO₂-bridged complexes has been observed for Pt(C₆H₅)(PEt₃)₂(COOH) in the solid state at ca. 100 °C to give the corresponding dimeric Pt complex with almost quantitative

(60) Gennaro, A.; Isse, A. A.; Vaianello, E. *J. Electroanal. Chem.* **1990**, *289*, 203–215.

coordinated through one of the oxygen atoms with a $\mu_2\text{-}\eta^2\text{-CO}_2$ configuration, where each dmb ligand is providing an electron to the bound CO_2 forming a carboxylate species.

In the one-electron-reduced species $\text{Re}(\text{dmb})(\text{CO})_3\text{S}$, the extra electron is located on the ligand and the equilibrium constant between the ligand- and metal-centered radicals ($\text{Re}(\text{dmb}^*)(\text{CO})_3\text{S}$ and $\text{Re}^*(\text{dmb})(\text{CO})_3$) is 10^{-4} . Thus the dimerization reaction of the ligand-centered radical via the metal radical is very slow compared to those of typical metal radicals of organometallic complexes. The reaction with CO_2 is also slow, since the binding of CO_2 requires an electron-rich metal center(s).

$[\text{Re}(\text{dmb})(\text{CO})_3]_2$ is unreactive toward CO_2 and $[\text{Re}(\text{dmb})(\text{CO})_3]_2(\text{CO}_2)$ only forms after the photodissociation of the Re dimer to $\text{Re}(\text{dmb}^*)(\text{CO})_3\text{S}$. In all the experiments we conducted with $[\text{Re}(\text{dmb})(\text{CO})_3]_2$ and CO_2 , we observed the formation of CO (a 25–50% yield based on $[\text{Re}]$) and final Re species (i.e., $[\text{Re}(\text{dmb})(\text{CO})_3]_2(\text{OCO}_2)$ and $\text{Re}(\text{dmb})(\text{CO})_3(\text{OC}(\text{O})\text{OH})$). In all the experiments we performed with $[\text{Re}(\text{dmb})(\text{CO})_3]_2(\text{CO}_2)$ under CO_2 , the formation of CO with similar yields and the same final products were confirmed. These results support the involvement of $[\text{Re}(\text{dmb})(\text{CO})_3]_2(\text{CO}_2)$ as a key intermediate in the reaction of $[\text{Re}(\text{dmb})(\text{CO})_3]_2$ with CO_2 . When ^{13}C is used, the final NMR spectrum indicates ^{13}C signals for only $\text{Re}(\text{dmb})(\text{CO})_3(\text{O}^{13}\text{C}(\text{O})\text{OH})$, $[\text{Re}(\text{dmb})(\text{CO})_3]_2(\text{O}^{13}\text{CO}_2)$, and ^{13}CO . Thus the reaction of $[\text{Re}(\text{dmb})(\text{CO})_3]_2(\text{CO}_2)$ with $^{13}\text{CO}_2$ takes place on the Re– CO_2 –Re moiety without any exchange with Re-bound CO. This result is quite different from that obtained by Hawecker et al.⁵

In photocatalytic systems, $\text{Re}(\text{dmb})(\text{CO})_3\text{S}$, the one-electron-reduced species of $\text{Re}(\text{dmb})(\text{CO})_3\text{Cl}$ formed by loss of Cl^- , would be expected to act as a catalyst in the reduction of CO_2 to CO by the formation of $[\text{Re}(\text{dmb})(\text{CO})_3]_2(\text{CO}_2)$ (and

$\text{Re}(\text{dmb})(\text{CO})_3\text{COOH}$ as a minor species). We believe that the route involving $[\text{Re}(\text{dmb})(\text{CO})_3]_2(\text{CO}_2)$ plays the major role. The presence of Cl^- , TEOA (or TEA), and water suppresses the formation of insoluble $[\text{Re}(\text{dmb})(\text{CO})_3](\text{OCO}_2)$ and allows $\text{Re}(\text{dmb})(\text{CO})_3\text{Cl}$ to reform. The liberation of CO via reaction of $\text{Re}(\text{dmb})(\text{CO})_3(\text{COOH})$ with a proton to form $\text{Re}(\text{dmb})(\text{CO})_4^+$ may be suppressed in the early stages of photochemical reactions; however, it may become an important route once significant amounts of TEOAH^+ or TEAH^+ are produced. Although formation of metal–formate complexes was reported in photochemical CO_2 reduction,^{4,5} we did not observe such complexes in our photochemical CO_2 reduction with $\text{Re}(\text{dmb})(\text{CO})_3\text{Cl}$ and TEA/DMF.

Acknowledgment. We thank Dr. Norman Sutin, Dr. Carol Creutz, Prof. Osamu Ishitani, Dr. Kazuhide Koike, and Prof. Kazuteru Shinozaki for valuable discussions. This work was performed at Brookhaven National Laboratory, funded under Contract DE-AC02-98CH10886 with the U.S. Department of Energy and supported by its Division of Chemical Sciences, Office of Basic Energy Sciences. S.K. acknowledges financial support from the Mombu-Kagaku-sho, Japan, as a fellow for research-in-abroad.

Supporting Information Available: Table of the reduction potentials of Re complexes and figures of UV–vis spectra of $\text{Re}(\text{dmb})(\text{CO})_3(\text{OTf})$, $[\text{Re}(\text{dmb})(\text{CO})_3]_2$, $[\text{Re}(\text{dmb})(\text{CO})_3]^-$, and $[\text{Re}(\text{dmb})(\text{CO})_3]_2$ in various solvents; plots of pseudo-first-order rate constant for decomposition of $[\text{Re}(\text{dmb})(\text{CO})_3]_2(\text{CO}_2)$ versus $[\text{CO}_2]$ in the dark and under continuous irradiation; and plot of the concentrations of various species versus time for the reactions of $\text{Re}(\text{dmb})(\text{CO})_3(\text{COOH})$ in DMF. This material is available free of charge via the Internet at <http://pubs.acs.org>.

JA035960A